Displays 34 (2013) 399–405

Contents lists available at ScienceDirect

Displays

journal homepage: www.elsevier.com/locate/displa

Mid-infrared characterization of thiophene-based thin polymer films

Akemi Tamanai *, Sebastian Beck, Annemarie Pucci

Kirchhoff Institute for Physics, University Heidelberg, Im Neuenheimer Feld 227, D-69120 Heidelberg, Germany

ARTICLE INFO

Article history:
Available online 30 August 2013

Keywords:
IR spectroscopy
IR ellipsometry
Thiophene-based polymer
Absorption
Dielectric function

ABSTRACT

Optical properties of seven regioregular poly(3-alkylthiophene) with different alkyl side chain lengths which are poly(3-butylthiophene-2,5-diyl) (P3BT), poly(3-pentylthiophene-2,5-diyl) (P3PT), poly(3-hexylthiophene-2,5-diyl) (P3HT), poly(3-heptylthiophene-2,5-diyl) (P3hept), poly(3-octylthiophene-2,5-diyl) (P3OT), poly(3-decylthiophene-2,5-diyl) (P3DT), and poly(3-dodecylthiophene-2,5-diyl) (P3DDT) have been studied in the mid-infrared (IR) spectral region by means of Fourier Transformation Infrared (FTIR) spectroscopy and IR spectroscopic ellipsometry (IRSE). Absorbance spectra obtained in this fingerprint region are potential to characterize the structures formed by organic molecules in thin films due to molecular vibrations in detail. In consequence, the vibrational absorption bands of these seven samples demonstrated that P3PT, P3HT, and P3hept exhibited very similar band profiles, in contrast, the stretching vibration of thiophene rings ($\approx$1465 cm^{-1}: C=C) underwent a blue shift in P3BT, P3OT, P3DT and P3DDT. The highest value of the real part (ε_1) of the complex dielectric constant was obtained from P3HT on both indium thin oxide (ITO) and silicon (Si) substrates whereas the imaginary part (ε_2) was directly affected by increasing in the alkyl side chain lengths in a frequency range around 3000 cm^{-1}. The optical properties of P3PT in the mid-IR region developed an affinity with those of P3HT. Thus, P3PT is particularly a suitable polymer active material candidate for high-performance devices.

1. Introduction

Thiophene-based conjugated semiconducting polymers such as regioregular P3ATs (P3BT, P3PT, P3HT, P3hept, P3OT, P3DT, and P3DDT) have been extensively studied for applications in optoelectronics such as organic field-effect transistors (OFET), organic light emitting diodes (OLED), and organic solar cells. One of the most well-known examples is P3HT as a *p*-type semiconductor material that has reached a charge carrier mobility of 0.1 $cm^2/V\,s$ [1,2]. In order to improve the mobility of P3HT, investigations on molecular orientations [3,4], crystallization processes [5], various sorts of solvents for a wet process sample preparation [6], and the characteristic effects of doping [7] have been carried out so far. Furthermore, after different alkyl side chain lengths of P3ATs have been developed, correlation of physical and optical properties with the alkyl side chain (C_nH_{2n+1}) length was analyzed in detail. P3AT/PCBM blend investigations revealed that as the alkyl side chain increased, solubility increased as well as photocurrents in general [8]. Conversely, absorption coefficient reduced as the alkyl side chain length increased due to less interspace between molecules [8]. The hole mobility of P3ATs was determined by output characteristics [9]. In this study, P3HT indicated the highest hole mobility value (1×10^{-2} $cm^2/V\,s$) followed by P3BT (1.2×10^{-3} $cm^2/V\,s$), P3OT (2.0×10^{-4} $cm^2/V\,s$), P3DT (6.6×10^{-5} $cm^2/V\,s$), and P3DDT (2.4×10^{-4} $cm^2/V\,s$) in virtue of the superlative self-assembling ability. An even–odd effect in number of monomers has been confirmed in poly(phenylene ethynylene) (PPE) and poly(phenylene-vinylene) systems [10], rigid-flexible polymers [11], and alkane thiol monolayers on gold [12]. These investigations revealed that the even–odd effect exceedingly influenced the transition temperatures, the molecular orientation angles, and the chain packing arrangements. Electrical properties of P3PT have been examined in UV and visible regions [13,14]. As a result, P3PT was presumed to be a possible candidate as a *p*-type semiconductor material since P3PT thin films exhibited a high degree of crystallinity with a π–π stacking distance, d_{010} of 3.74 Å [14] which was very close to that of P3HT (3.8 Å) [15].

In this paper, we examined the optical properties of seven regioregular P3ATs with alkyl side chain of C_nH_{2n+1}: n = 4, 5, 6, 7, 8, 10, 12 (P3BT, P3PT, P3HT, P3hept, P3OT, P3DT, and P3DDT), respectively, by means of FTIR spectroscopy in a frequency range between 800 and 3300 cm^{-1}. FTIR spectroscopy provides detailed information of each molecular bonding since absorption/transmission spectra represent the fingerprint of a material along with absorption peaks that are generated by vibrational transitions of atomic bonds. In addition, the dielectric properties of odd-num-

* Corresponding author. Tel.: +49 6221549894.
E-mail address: akemi@kip.uni-heidelberg.de (A. Tamanai).

0141-9382
http://dx.doi.org/10.1016/j.displa.2013.08.005

bered P3hept and P3PT on Si and ITO substrates in the fingerprint region have been derived by the use of IRSE which is a technique that measures the variations in the polarization state of an incident light before and after reflection on a surface of a target material. Hereby accurate film thicknesses of thin films and their complex dielectric functions can be determined. The dielectric function of P3HT (even-numbered) has been derived as well in order to make a comparative study to odd-numbered materials. Moreover the surface roughness of all seven P3AT films was analyzed by atomic force microscopy (AFM).

2. Experiment

2.1. FTIR spectroscopy

FTIR spectrometers (Bruker IFS 66 v/S & Vertex 80 V) with a Deuterated Triglycine Sulfate (DTGS) detector were used for the measurements of IR spectra (absorbance) in a frequency range between 450 and 5500 cm^{-1}. All the absorbance measurements were carried out with a resolution of 4 cm^{-1} and a sample scan time of 1000 scans under a vacuum pressure between 2 and 5 mbar.

2.2. IRSE

ψ and Δ spectrum measurements were performed in a frequency range between 333 and 6000 cm^{-1} with an angle of incidence of 40°, 50°, 60°, and 70° under normal pressure by a rotating compensator IR ellipsometer from J. A. Woollam Co., Inc. (IR-VASE). In order to obtain the dielectric functions and the precise thickness of a thin film, ψ and Δ measured spectra were fitted based on an optical model by the use of WVASE32 software [37]. Fundamentally, these parameters are related to the Fresnel reflection coefficient r_p (p-polarized) and r_s (s-polarized) which determines the complex reflectance ratio ρ. Thus the complex reflectance ratio ρ can be described as:

$$\rho = \frac{\tilde{r}_p}{\tilde{r}_s} = \tan(\psi)e^{i\Delta} \tag{1}$$

where $\tan\psi$ denotes the relative amplitude attenuation while Δ represents the phase shift of the p and s linearly polarized components due to reflection.

Oscillations of atomic bonds are usually observed in the IR range due to a change in the dipole moment. The optical properties of an isotropic layer can then be expressed as a summation of Lorentzian oscillators

$$\varepsilon(\omega) = \varepsilon_1 + i\varepsilon_2 = \varepsilon_\infty + \sum_{j=1}^{N} \frac{s_j\omega_j^2}{\omega_j^2 - \omega^2 i\gamma_j\omega} \tag{2}$$

where ε_1 is the real part of the dielectric function, ε_2 the imaginary part of the dielectric function, ε_∞ a real constant, N the number of oscillators, s_j an amplitude of the jth oscillator, γ_j the damping factor of the jth oscillator, ω_j the broadening parameter related to the jth oscillator, and ω the resonance frequency.

A film thickness can be determined by interferences between light reflected from different surfaces:

$$d = \beta \frac{\lambda}{2\pi\sqrt{N_2^2 - N_1^2\sin^2(\Phi_1)}} \tag{3}$$

where d is the film thickness, β the phase factor, λ the wavelength of light, N_1 the refractive index of surroundings, N_2 the refractive index of a film, and ϕ_1 the angle of incidence [16,17].

2.3. Sample preparation

We have acquired commercially available regioregular P3BT, P3PT, P3hept, P3OT, P3DT, and P3DDT from Rieke Metals Inc. [18], and P3HT (Lisicon SP001; molecular weight (MW) 43600 and regioregularity (RR ≈ 95.9)) from Merck KGaA. It has been reported that solubility and field-effect mobilities of P3HT films were improved by dint of high boiling point (BT) solvents such as 1,2,4-Trichlorobenzene (BP: 213.5°) and 1,2-Dichlorobenzene (BP: 180°) due to progress of self-assembly [6,19]. Thus we selected 1,2-Dichlorobenzene (Merck KGaA) as a solvent for this investigation. Weight ratio percentage concentration of all the solutions was fixed to 2%. The solutions were placed on a hot plate with a temperature between 60 and 70 °C for 30 min so as to dissolve them thoroughly. All samples were prepared by spin coating process (SPS Europe: SPIN150-NPP) at rotation speed of 4000 rpm on Si wafers and ITO coated glass substrates (SiO_2 barrier coating was applied on polished soda lime float glass, and the ITO, resistance 7 Ω/sq, was deposited on it, VisionTek Systems Ltd. for both FTIR and IRSE measurements. As additional information, Drude metal modeling was employed for fitting the optical data of the ITO coated glass substrates.

3. Results and discussions

3.1. FTIR absorption spectroscopy

Absorbance spectra of P3BT, P3PT, P3hept, P3OT, P3DT, and P3DDT in the frequency range between 800 and 3300 cm^{-1} are shown in Fig. 1. Strong molecular absorption bands can be seen in the frequency range between 800 and 1600 cm^{-1} and 2800 and 3100 cm^{-1}. The films were fabricated nearly equivalent in thickness (≈66 ± 2 nm) so as to compare the absorption strength of each sample. Table 1 summarizes the characteristic mid-IR bands of 7 materials, and the film thickness of each film is described in Table 2. The film thickness was determined by use of a Dektak (Veeco Dektak 150) and IRSE for Si and ITO substrates, respectively. The stretching vibrations of the thiophene rings were detected in the frequency range between 819 and 834 cm^{-1} [28]. The absorption peak around 1378 cm^{-1} was contributed by the methyl deformation [29]. The symmetric C=C stretching vibration bands of the thiophene rings were shown in the range between 1456 and 1467 cm^{-1} [28]. On the other hand, the antisymmetric C=C stretching vibration bands of the rings appeared around 1510 cm^{-1} [28]. These four absorption bands were related to the stretching vibration modes of the thiophene rings, and the symmetric C=C vibration band around 1465 cm^{-1} underwent a blue shift in P3BT, P3OT, P3DT and P3DDT compared with the P3PT, P3HT, and P3hept. In addition, P3PT was the one to show the strongest absorption peaks at 819 and 1456 cm^{-1} among all those 7 materials. Absorption peaks located between 2800 and 3000 cm^{-1} were contributed from the alkyl side chains. Absorptions around 2855 and 2925 cm^{-1} were caused by the symmetric and antisymmetric CH_2 stretching vibrations, respectively [30]. The antisymmetric CH_3 stretching vibration band took place around 2956 cm^{-1} [30] whereas the absorption peak around 3056 cm^{-1} was associated with the C—H stretching vibration band of the thiophene rings [28]. Systematic and unsystematic changes in the vibrational modes corresponding to the symmetric and antisymmetric CH_2 as well as the antisymmetric CH_3 were observed as the alkyl side chain length was varied as shown in Fig. 1. A systematic red[1] shift of both symmetric and antisymmetric CH_2 stretching

[1] For interpretation of color in Fig. 1, the reader is referred to the web version of this article.

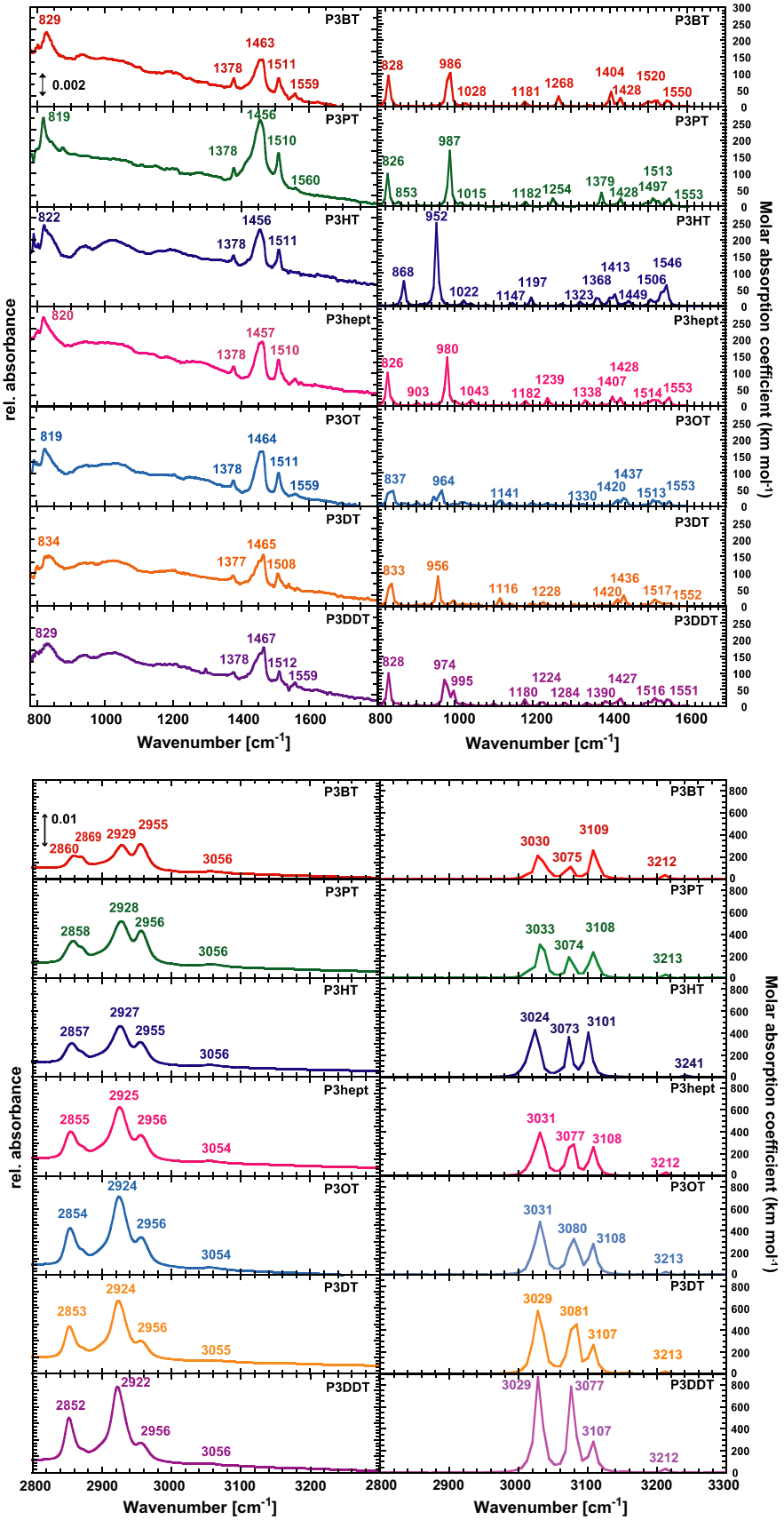

Fig. 1. IR absorbance spectra of the seven P3AT thin layers on Si substrates (right) together with the molar absorption coefficient (km mol^{-1}) spectra obtained by the DFT calculations (left). Top: a frequency range between 700 and 1800 cm^{-1}. Bottom: a frequency range between 2800 and 3300 cm^{-1}. The numbers in each plot designate the absorption peak positions in the spectra. Intensities are normalized to Si substrate spectrum.

Table 1
Characteristic absorption bands of the seven P3AT samples.

Wavenumber (cm^{-1})							
P3BT	P3PT	P3HT	P3hept	P3OT	P3DT	P3DDT	Assignment
829 (828)	819 (826)	822 (767)	820 (826)	819 (837)	834 (833)	829 (828)	Thiophene ring, C—H out-of-plane [28]
1378 (1349)	1378 (1378)	1378 (1368)	1378 (1380)	1378 (1371)	1377 (1372)	1378 (1369)	CH_3 methyl deformation [29]
1463 (1439)	1456 (1438)	1456 (1438)	1457 (1439)	1464 (1438)	1465 (1438)	1467 (1441)	Thiophene ring, sym. C=C [28]
1511 (1551)	1510 (1551)	1511 (1550)	1510 (1551)	1511 (1552)	1508 (1552)	1512 (1551)	Thiophene ring, antisym. C=C [28]
2860 (3029)	2858 (3030)	2857 (3023)	2855 (3029)	2854 (3031)	2853 (3025)	2852 (3026)	CH_2 sym. Stretching [30]
2929 (3073)	2928 (3075)	2927 (3073)	2925 (3076)	2924 (3083)	2924 (3074)	2922 (3078)	CH_2 antisym. Stretching [30]
2955 (3108)	2956 (3105)	2955 (3099)	2956 (3105)	2956 (3105)	2956 (3104)	2956 (3105)	CH_3 antisym. Stretching [30]
3056 (3211)	3056 (3211)	3056 (3242)	3054 (3211)	3054 (3214)	3055 (3214)	3056 (3211)	Thiophene ring, C—H stretching [28]

Note: All the absorbance peak position values are obtained from absorbance spectra whereas the wavenumbers in parentheses are calculated values from DFT.

Table 2
The surface roughness (R_q) of the seven P3AT samples.

Samples	Surface roughness (R_q)	Substrate type	Film thickness (nm)	Usage
P3BT	1.97	Si	65.9	FTIR
P3PT	5.77	Si	66.6	FTIR
P3HT	4.60	Si	66.8	FTIR
P3hept	1.81	Si	65.9	FTIR
P3OT	1.31	Si	65.7	FTIR
P3DT	0.58	Si	68.3	FTIR
P3DDT	0.82	Si	64.7	FTIR
P3PT	7.42	ITO	76.2 ± 0.2	IRSE
P3HT	9.47	ITO	55.4 ± 0.2	IRSE
P3hept	2.21	ITO	41.6 ± 0.2	IRSE

vibration bands was observed as the alkyl side chain length increased. Unlike the systematic peak shifts, unsystematic tendencies have emerged from this frequency region with respect to the absorption strength. P3BT < P3hept < P3HT < P3PT < P3DT < P3OT < P3DDT is designated in order of increasing the absorption strength of both symmetric and antisymmetric CH_2 stretching vibration bands as well as P3BT < P3PT < P3HT < P3OT < P3hept < P3DT < P3DDT for the antisymmetric CH_3 stretching ones. Both symmetric and antisymmetric CH_2 stretching bands of P3DDT were approximately a factor of 3 stronger than those of P3BT. In any cases, P3BT indicated the lowest absorption strength whereas the strongest one was obtained from P3DDT. Additionally, a clear shoulder was able to be seen at slightly higher wavenumbers (around 2869 cm^{-1}) in contrast to the symmetric CH_2 stretching vibration band. This shoulder correlated with the antisymmetric CH_3 stretching vibration and diminishes as the alkyl side chain length increased. Thus it directly reflected to the absorption strength around 2955 cm^{-1}. The absorption strength was not influenced by the alkyl side chain length systematically in the chain length between $n = 5$ (P3PT) and $n = 10$ (P3DDT).

The degree of crystallinity strongly depends on the spin speed. Higher crystallinity as well as low defects in its crystal system can be achieved with a slower evaporation rate in general [31,32]. Yazawa et al. reported that the C—H out-of-plane vibration mode located in the frequency region between 850 cm^{-1} and 800 cm^{-1} is delicately influenced by the crystalline structure [33]. As shown in Fig. 1, the absorption peak contributed by the C—H out-of-plane vibration of P3PT in particular is rather prominent compared with that of other P3AT samples. Although the high spin speed (4000 rpm) was applied for the film fabrication, the evaporation rate was not so high due to the use of high BT solvent. Thus some P3AT samples in the remaining solvent could have enough time to extent local crystallinity. Especially, a net shear force (the centrifugal forces (outward) and the surface tension (inward)) with regard to the polymer chain is strong enough to stretch the chains from tangled condition [34]. Therefore, P3AT samples with relatively shorter side chain lengths might show the slightly higher absorption peaks.

We performed density functional theory (DFT) monomer calculations for these seven samples by making use of Gaussian 09W with the B3LYP functional and a 6-31G basis set as well. The peak positions of the thiophene ring vibration bands were reproduced well by the DFT calculations compared to those of the alkyl side chain vibration bands which underwent a blue shift in the DFT simulations. The difference between the DFT and the measured spectra might be caused by a disparity in the number of molecules constituting a thin layer together with molecular orientation. The molecular orientation in the experiments is influenced by many factors such as type of solvent [19], surface roughness of substrate [20,21], and substrate surface treatment e.g. metal deposition [22] which directly reflect IR band profiles. In addition, the morphology of each molecule is closely related to interactions and molecular structures. In the visible region, an average tilt angle of the electronic transition dipole moment with respect to the substrate surface normal can be inspected. For example, the absorption peak from the C=C π^* transition shows a clear systematic change with the incident angle which governs the average conjugated plane orientation. The π^* orbital extends orthogonally to the π-conjugated plane of P3HT, for instance; therefore, the P3HT takes an "edge-on" orientation [30]. On the other hand, the degree of molecular orientation of each segment by the use of polarized light can be investigated with vibrational spectroscopy in mid-IR spectral region as shown in Fig. 1. Applying the ratio of the absorbance peaks (A_p/A_s) measured by both *p*- and *s*-polarized light at Brewster angle of substrate, the molecular orientation of each fragment can be determined [30]. The tilt angles of P3HT films fabricated by spin-casting with different sorts of solvents were between 57° and 60° as well as 59° by drop-cast P3HT film [32]. Likewise, Hao et al. took the thiophene ring orientation into account, and the measured average tilt angles of P3HT films were reported as 62°, 72°, and 70° for a spin coating process with high rotating speed, low speed, and dip coating, respectively [35,36]. Detailed analysis of molecu-

lar orientations of each P3AT samples should be a next task for further investigations.

Throughout the whole frequency range, we perceived that P3PT, P3HT, and P3hep resembled each other closely in mid-IR band profiles, particularly, the absorption peak positions due to the thiophene ring stretching vibrations.

3.2. IRSE

By the FTIR spectroscopic absorbance measurements of P3AT samples, we have detected a great similarity among the mid-IR band profiles of P3PT, P3HT, and P3hept. Thus a further study of these three samples has been performed for revealing the optical

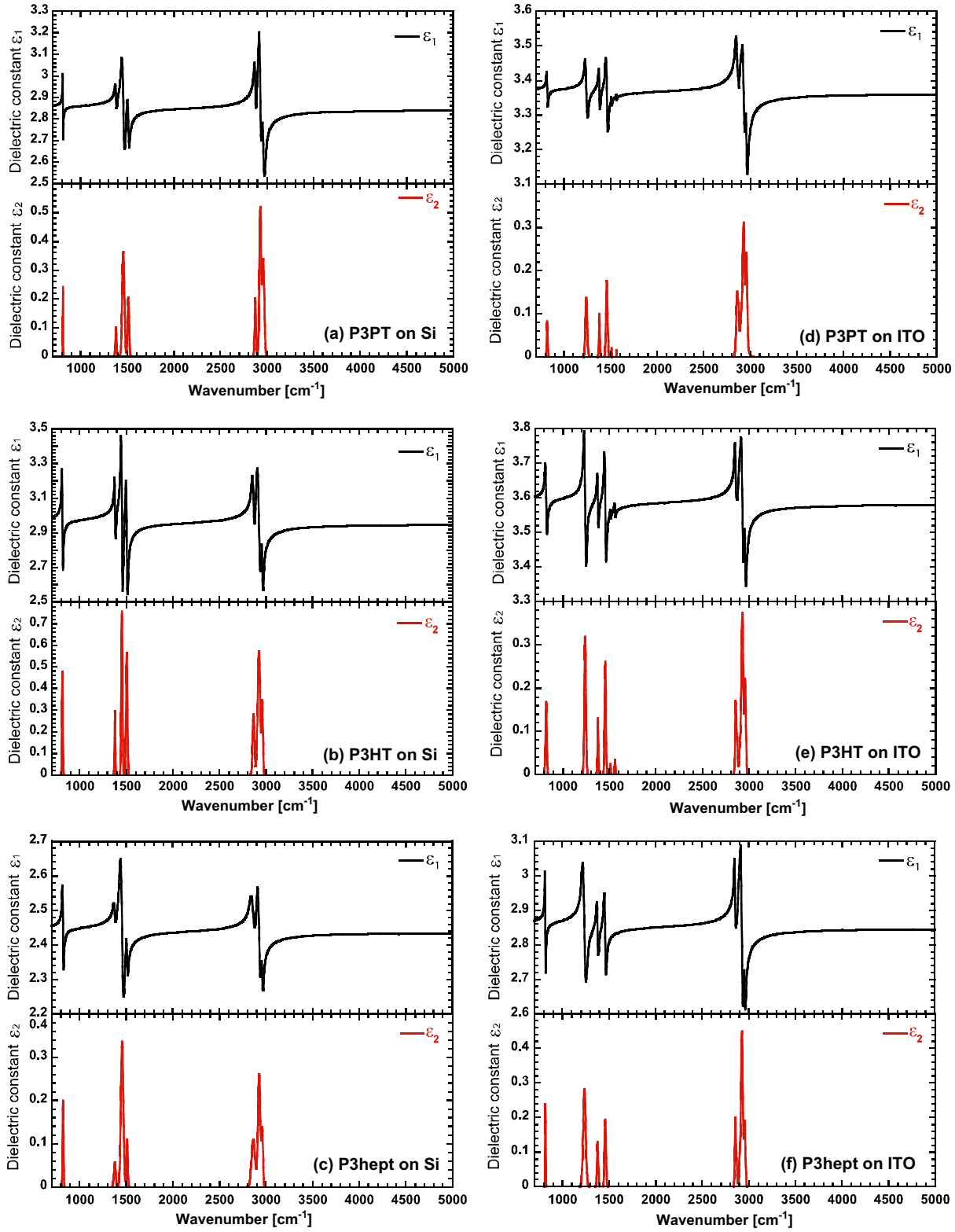

Fig. 2. Dielectric constants of three P3AT thin layers on Si and ITO substrates. Left column: (a) P3PT, (b) P3HT, and (c) P3hept on Si substrates. Right column: (d) P3PT, (e) P3HT, and (f) P3hept on ITO substrates. Note: each plot has a different ordinary scale.

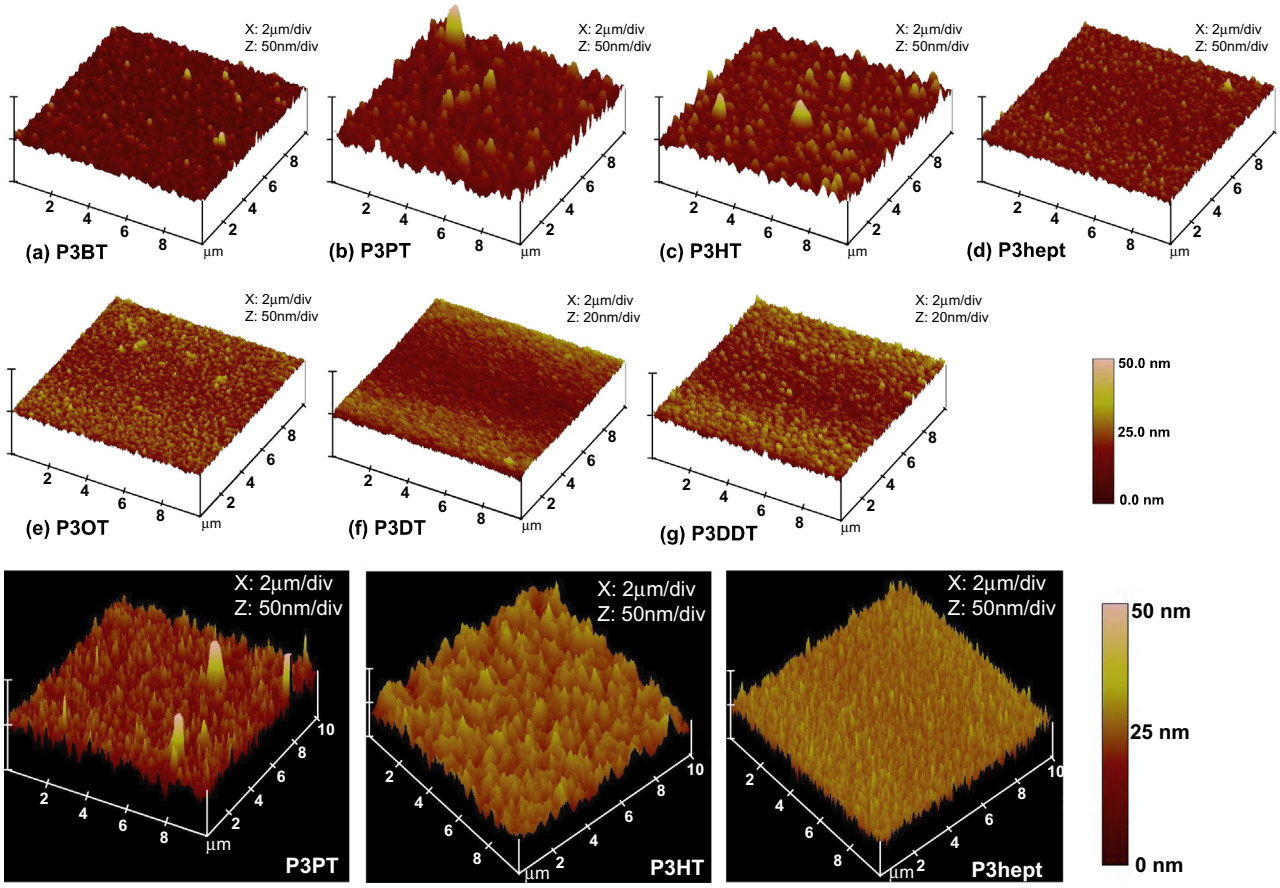

Fig. 3. AFM topography images of the seven P3AT samples. Top: The thin layers of (a) P3BT, (b) P3PT, (c) P3HT, (d) P3hept, (e) P3OT, (f) P3DT, and (g) P3DDT on Si substrates. Bottom: P3PT (left), P3HT (center), and P3hept (right) thin layers on ITO substrates. All images are 10 × 10 μm.

properties in detail by means of IRSE. Variable angle measurements did not reveal any anisotropic behavior. An isotropic complex dielectric function was derived from measured ψ and Δ spectra for the real and imaginary parts of P3PT, P3HT and P3hept on Si and ITO substrates, see Fig. 2. The real part of the dielectric function (ε_1) of every layer on ITO substrates was approximately 10–17% higher than in the case of Si substrates. Additionally, the real part of the highest dielectric constant was obtained from P3HT with both Si (3.46) and ITO (3.79) substrates. Maximum values ε_1 are reached for maximum in oscillator strength as well as ε_∞. On the other hand, the CH_2 antisymmetric stretching absorption (around 2925 cm^{-1}) was enhanced as the alkyl side chain length increased; thus the imaginary part (ε_2) of the dielectric constant of P3hept appeared stronger than in the case of P3PT and P3HT on ITO substrate. However, this tendency could not be applied to the Si substrate case. The imaginary part of the dielectric function of P3hept was the weakest among them. The cause of this discrepancy may come from the substrate material type and surface roughness of the substrate which controls the molecular orientation (e.g. molecular angles) of the samples. The relative peak heights or strengths (Figs. 1 and 2) indicate the disparity in molecular orientation on ITO and Si substrates. In comparison to the absorption strengths due to methyl deformation of P3hept on Si (Fig. 1) and ITO (Fig. 2f) substrates, it is clearly seen that this vibration dipole is more perpendicular to ITO substrate. In order to improve the strength of absorption, a degree of self-assembly is one of important factors [23]. Particularly solution-processed thin layers strongly depend on the kind of molecule used and solvents as well as that compatibility with substrates [24,25].

There is a correlation among the film thickness, surface roughness, and crystallinity which directly reflects dielectric properties. A study of thin polymer films (parylene $C(C_8H_7Cl)_n$) demonstrated that the film roughness was decreased in a semicrystalline material as the film crystallinity diminished [26] whereas the X-ray and electron diffraction patterns clarified the higher degree of edge-on orientation of the P3AT polymer crystal formation with a reduction in the alkyl side chain length which provided higher mobility than in the case of plane-on orientation [27]. This disparity in the orientation affects the surface roughness. If the longer alkyl side chains are oriented perpendicular to a substrate, the surface roughness should increase more than the shorter chains. Our AFM (Newport Multimode™ Model 401) topography analysis shown in Fig. 3 revealed that the surface roughness was decreased with increasing in the alkyl side chain length except the shortest (P3BT) and longest (P3DDT) alkyl side chain cases. The surface roughness (the root mean square average, R_q) value of P3AT films on ITO substrates was higher than that of the films on Si substrates (Table 2). R_q values of P3PT on Si substrate (5.77 nm) and P3HT on ITO substrate (9.47 nm) indicated the highest values compared to other P3AT samples which had the surface roughness of less than 2.2 nm. A principle cause is related to the solubility which controls the undissolved residuals of the polymer samples in solvent. In fact, the solubility of polymers was enhanced with increasing in the alkyl side chain length [8]. The topography images exhibited some high spots which could be associated with the undissolved remnants in the solvent.

4. Conclusion

We have investigated the optical properties of P3AT thin films with various alkyl side chain lengths (C_nH_{2n+1}: n = 4, 5, 6, 7, 8, 10,

12) by dint of FTIR spectroscopy and IRSE in a frequency range between 450 and 5500 cm^{-1}. This experimental approaches revealed that a blue shift of the stretching vibration of the thiophene ring ($\approx$1465 cm^{-1}: C=C) was observed in P3BT, P3OT, P3DT and P3DDT compared to P3PT, P3HT, and P3hept whereas P3PT, P3HT, and P3hept thin layers exhibited very similar band profiles. A systematic red shift of both symmetric and antisymmetric CH_2 stretching vibration bands in the frequency range between 2920 and 2955 cm^{-1} was detected and unsystematic tendencies appeared concerning the absorption strength with increasing in the alkyl side chain length. With respect to the surface roughness of each sample, it decreased sharply from the alkyl side chain $n = 4$ (P3hept) up to $n = 12$ (P3DDT). via the IRSE measurements, the highest value of the real part of the dielectric function (ε_1) was derived by ψ and Δ spectra of P3HT on both Si and ITO substrate cases. On the other hand, the imaginary part (ε_2) of the complex dielectric function in frequency around 3000 cm^{-1} augmented with increasing in alkyl side chain length. The dielectric properties of P3PT in the mid-IR region developed a resemblance with those of P3HT. P3PT can be a promising candidate material in order to improve the performance of organic electronic devices.

Acknowledgements

We are grateful to Dipl.-Ing. C. Leonhard, Dr. N. Traut, Dr. K.C. Deing (Merck) and Dipl.-Phys. M. Alt (KIT) for their technical support at iL. We express to Dr. Gael Rouille at FSU Jena our gratitude for insightful comments for theoretical simulations, Dr. S. Wetzel at KIP for his technical support of AFM, and Dipl.-Phys. J. Trollmann at KIP for proofreading. We are thankful to Dr. T. Tiwald at J.A. Woollam Co., Inc. and Mr. Th. Wagner at LOT for their assistance regarding the IRSE modeling. This research has been financially supported by the Bundesministerium für Bildung und Forschung (BMBF) via the projects Polytos and Mesomerie.

References

[1] Z. Bao, A. Dodabalapur, A.J. Lovinger, Soluble and processable regioregular poly(3-hexylthiophene) for thin film field-effect transistor applications with high mobility, Appl. Phys. Lett. 26 (1996) 4109.
[2] H. Sirringhaus, N. Tessler, R.H. Friend, Integrated optoelectronic devices based on conjugated polymers, Science 280 (1998) 1741.
[3] H. Sirringhaus, P.J. Brown, R.H. Friend, M.M. Nielsen, K. Bechgaard, B.M.W. Langeveld-Voss, A.J.H. Spiering, R.A.J. Janssen, E.W. Meijer, P. Herwig, D.M. de Leeuw, Two-dimensional charge transport in self-organized, high-mobility conjugated polymers, Nature 401 (1999) 685.
[4] D. Choi, S. Jin, Y. Lee, S.H. Kim, D.S. Chung, K. Hong, C. Yang, J. Jung, J.K. Kim, M. Ree, C.E. Park, Direct observation of interfacial morphology in poly(3-hexylthiophene) transistors: relationship between grain boundary and field-effect mobility, ACS Appl. Mater. Interfaces 2 (2010) 48.
[5] S. Malik, A.K. Nandi, Crystallization mechanism of regioregular poly(3-alkyl thiophene)s, J. Polym. Sci. Pol. Phys. 40 (2002) 2073.
[6] J.F. Chang, B. Sun, D.W. Breiby, M.M. Nielsen, T.I. Sölling, M. Giles, I. McCulloch, H. Sirringhaus, Enhanced mobility of poly(3-hexylthiophene) transistors by spin-coating from high-boiling-point solvents, Chem. Mater. 16 (2004) 4772.
[7] Y.H. Kim, D. Spiegel, S. Hotta, A.J. Heeger, Photoexcitation and doping studies of poly(3-hexylthienylene), Phys. Rev. B 38 (1988) 5490.
[8] L.H. Nguyen, H. Hoppe, T. Erb, S. Günes, G. Gobsch, H.S. Sariciftci, Effects of annealing on the nanomorphology and performance of poly(alkylthiophene): fullerene bulk-heterojunction solar cells, Adv. Funct. Mater. 17 (2007) 1071.
[9] A. Babel, S.A. Jenekhe, Alkyl chain length dependence of the field-effect carrier mobility in regioregular poly(3-alkylthiophene)s, Synth. Met. 148 (2005) 169.
[10] D.A.M. Egbe, C. Ulbricht, T. Orgis, B. Carbonnier, T. Kietzke, M. Peip, M. Metzner, M. Gericke, E. Birckner, T. Pakula, D. Neher, U.W. Grummt, Odd-even effects and the influence of length and specific positioning of alkoxy side chains on the optical properties of PPE–PPV polymers, Chem. Mater. 17 (2005) 6022.
[11] B. Carbonnier, A.K. Andreopoulou, T. Pakula, J.K. Kallitsis, Effect of structural parameters on the supramolecular organization of rigid-flexible polymers, Macromol. Chem. Phys. 206 (2005) 66.
[12] L. Ramin, A. Jabbarzadeh, Odd–even effects on the structure stability, and phase transition of alkanethiol self-assembled monolayers, Langmuir 27 (2011) 9748.
[13] W. Czerwiński, L. Kreja, M. Chrzaszcz, A. Kazubski, Structural and electrical properties of soluble conducting poly (3-pentylthiophene), J. Mater. Sci. 29 (1994) 1191.
[14] P.T. Wu, H. Xin, F.S. Kim, G. Ren, S.A. Jenekhe, Regioregular poly(3-pentylthiophene): synthesis self-assembly of nanowires, high-mobility field-effect transistors, and efficient photovoltaic cells, Macromolecules 42 (2009) 8817.
[15] S. Samitsu, T. Shimomura, S. Heike, T. Hashizume, K. Ito, Effective production of poly(3-alkylthiophene) nanofibers by means of whisker method using anisole solvent: structural optical, and electrical properties, Macromolecules 41 (2008) 8000.
[16] H.G. Tompkins, E.A. Irene, Handbook of Ellipsometry, first ed., William Andrew, NY, 2005.
[17] H. Fujiwara, Spectroscopic Ellipsometry: Principles and Applications, first ed., John Wiley, Chichester, 2007.
[18] T.A. Chen, X. Wu, R.D. Rieke, Regiocontrolled synthesis of poly(3-alkylthiophenes) mediated by rieke zinc: their characterization and solid-state properties, J. Am. Chem. Soc. 117 (1995) 233.
[19] M. Ichikawa, Manufacturing organic transistors by using a spin coating, in: Y. Ohmori (Ed.), Recent Progress in Fabrication of Organic Thin Film and Device Applications, CMC Publishing Co., Ltd., Tokyo, 2008, pp. 88–94.
[20] H. Peisert, I. Biswas, L. Zhang, M. Knupfer, M. Hanack, D. Dini, D. Batchelor, T. Chassé, Molecular orientation of substituted phthalocyanines: influence of the substrate roughness, Surf. Sci. 600 (2006) 4024.
[21] J. Deng, Y. Baba, T. Sekiguchi, N. Hirao, M. Honda, Effect of substrates on the molecular orientation of silicon phthalocyanine dichloride thin films, J. Phys.: Condens. Matter 19 (2007) 196205.
[22] K. Kanai, T. Ikame, Y. Ouchi, K. Seki, Molecular orientation and electronic structure of 11,11,12,12-tetracyanonaphtho-2,6-quinodimethane vacuum-deposited on metal substrates: charge transfer, complexation, and potassium doping, J. Appl. Phys. 105 (2009) 023703.
[23] T. Yamamoto, Molecular assembly and properties of polythiophenes, NPG Asia Mater. 2 (2010) 54.
[24] R.G. Nuzzo, D.L. Allara, Adsorption of bifunctional organic disulfides on gold surfaces, J. Am. Chem. Soc. 105 (1983) 4481.
[25] Y. Gu, Z. Lin, R.A. Butera, V.S. Smentkowski, D.H. Waldeck, Preparation of self-assembled monolayers on InP, Langmuir 11 (1995) 1849.
[26] A. Kahouli, Effect of film thickness on structural, morphology, dielectric and electrical properties of parylene C films, J Appl. Phys. 112 (2012) 064103.
[27] Y.D. Park, D.H. Kim, Y. Jang, J.H. Cho, M. Hwang, H.S. Lee, J.A. Lim, K. Cho, Effect of side chain length on molecular ordering and field-effect mobility in poly(3-alkylthiophene) transistors, Org. Electron. 7 (2006) 514.
[28] S. Hotta, S.D.D.V. Rughooputh, A.J. Heeger, F. Wudl, Spectroscopic studies of soluble poly(3-alkylthienylenes), Macromolecules 20 (1987) 212.
[29] H. Wei, L. Scudiero, H. Eilers, Infrared and photoelectron spectroscopy study of vapor phase deposited poly(3-hexylthiophene), Appl. Surf. Sci. 255 (2009) 8593.
[30] D.M. DeLongchamp, R.J. Kline, D.A. Fischer, L.J. Richter, M.F. Toney, Molecular characterization of organic electronic films, Adv. Mater. 23 (2011) 319.
[31] H. Yang, T.J. Shin, L. Yang, K. Cho, C.Y. Ryu, Z. Bao, Effect of mesoscale crystalline structure on the field-effect mobility of regioregular poly(3-hexyl thiophene) in thin-film transistors, Adv. Funct. Mater. 15 (2005) 671.
[32] P.K.-H. Ho, L.-L. Chua, M. Dipankar, X. Gao, D. Qi, A.T.-S. Wee, J.-F. Chang, R.H. Friend, Solvent effects on chain orientation and interchain π-interaction in conjugated polymer thin films: direct measurements of the air and substrate interfaces by near-edge X-ray absorption spectroscopy, Adv. Mater. 19 (2007) 215.
[33] K. Yazawa, Y. Inoue, T. Yamamoto, N. Asakawa, Twist glass transition in regioregulated poly(3-alkylthiophene), Phys. Rev. B 74 (2006) 094204.
[34] I.M. Craig, C.J. Tassone, S.H. Tolbert, B.J. Schwartz, Second-harmonic generation in conjugated polymer films: a sensitive probe of how bulk polymer crystallinity changes with spin speed, J. Chem. Phys. 133 (2010) 044901.
[35] X.T. Hao, T. Hosokai, N. Mitsuo, S. Kera, K. Mase, K.K. Okudaira, N. Ueno, Electronic density tailing outside π-conjugated polymer surface, Appl. Phys. Lett. 89 (2006) 182113.
[36] X.T. Hao, T. Hosokai, N. Mitsuo, S. Kera, K.K. Okudaira, K. Mase, N. Ueno, Control of the interchain π–π interaction and electron density distribution at the surface of conjugated poly(3-hexylthiophene) thin films, J. Phys. Chem. B 111 (2007) 10635.
[37] R.A. Synowicki, Spectroscopic ellipsometry characterization of indium thin oxide silm microstructure and optical constants, Thin Solid Films 313–314 (1998) 394.